The Astronomical Journal, 166:261 (9pp), 2023 December https://doi.org/10.3847/1538-3881/ad0734

Variability in Early Post-main-sequence Stars in Globular Cluster NGC 3201

D. Ulloa-Solís[1], C. C. Cortés[2], S. Villanova[1], Á. Llancaqueo Albornoz[1], J. A. Ahumada[3], and C. Parisi[3,4]
[1] Departamento de Astronomía, Casilla 160-C, Universidad de Concepción, Concepción, Chile
[2] Departamento de Tecnologías Industriales, Faculty of Engineering, Universidad de Talca, Merced 437, Curicó, Chile
[3] Observatorio Astronómico, Universidad Nacional de Córdoba, Laprida 854, 5000, Córdoba, Argentina
[4] Instituto de Astronomía Teórica y Experimental (CONICET-UNC), Laprida 854, 5000, Córdoba, Argentina
Received 2023 June 16; revised 2023 October 24; accepted 2023 October 25; published 2023 November 23

Abstract

In this paper we study stellar variability in the globular cluster NGC 3201 in the magnitude range $V = 16–17$, corresponding to the subgiant branch and blue stragglers region of the cluster. Our aim is to expand the sample of new type of variables with low amplitude and a short period found in previous papers. We used observations obtained at the Complejo Astronómico El Leoncito. We applied statistical tests and analyzed periodograms obtained by generalized Lomb–Scargle and phase dispersion minimization methods. We found five stars considered as variables and one as a possible variable. According to their periods (fluctuating between 0.33 and 0.57 days), amplitudes (between 0.03 and 0.87 V magnitudes), the position in the color–magnitude diagram, and the shape of their phased light curves, they do not resemble any known variable star. Because stellar variability could be produced by more than one process, we propose to complement this work with a spectroscopic analysis to confirm our results.

Unified Astronomy Thesaurus concepts: Globular star clusters (656); Variable stars (1761); Evolved stars (481)

1. Introduction

Among the various astronomical objects present in the Milky Way, globular clusters (GCs) have been and are still one of the most important components since their studies over the last century have made essential contributions to our understanding of stellar evolution and also the structure of our Galaxy. Being one of the oldest known objects in the Universe, GCs have been objects of deep analysis. They were believed to be the best example of single stellar population, but chemical analysis on stars of several GCs, with the most notorious works being the studies made by Gratton et al. (2004) and Carretta et al. (2009a, 2009b), disproved such claims showing that they display inhomogeneities in their light element content, Ruprecht 106 beeing the only exception known (Kaluzny et al. 2016). Regardless, GCs still prove to be indispensable structures that require careful and precise study to unravel the history of the Milky Way.

One interesting cluster is NGC 3201 (C1015−461), being at low galactic latitude ($b = +8\overset{\circ}{.}64$), at a distance of ∼4.9 kpc, and located at $\alpha = 10^{h}17^{m}36\overset{s}{.}82$, $\delta = -46°24'44''9$ (J2000; Harris 1996). Several studies have been performed on this object due to the controversy about its [Fe/H] content since it was debated if its spread is intrinsic or due to some analysis issue (see, for example, Gonzalez & Wallerstein 1998; Muñoz et al. 2013; Simmerer et al. 2013; Mucciarelli et al. 2015). Furthermore, NGC 3201 is also known for its rich variable star population, having 121 targets according to the 2012 update of the Catalogue of Variable Stars in Globular Clusters (Clement et al. 2001), as well as containing several RGB stars with low-amplitude light variations (Layden & Sarajedini 2003). Many works have been published in order to study its variables (e.g., Layden & Sarajedini 2003; Arellano Ferro et al. 2014; Kaluzny et al. 2016; Llancaqueo Albornoz et al. 2021). As a further note on the topic of low-amplitude variable stars, there is knowledge about stars that display not only such low amplitudes but also large periods, being known as pulsating red giants, the classification having been provided by Olin Eggen in a series of papers (e.g., Eggen 1973, 1977).

Recent studies have brought results showing that variability and metallicity might be related in some way, starting with the chemical abundance analysis in the bulge GC NGC 6528 by Muñoz et al. (2018), where the authors found a red giant variable star ($P = 0.26$ days, and $A = 0.05$ mag in infrared), with an [Fe/H]$= -0.55$, way lower than the [Fe/H] values of the other six stars of his sample ([Fe/H] $= -0.14 \pm 0.03$ on average). They analyzed their period using the photometric data from the VVV survey (Minniti et al. 2010; Saito et al. 2012). After this first result Llancaqueo Albornoz et al. (2021) revisited NGC 3201 by analyzing 17 giant stars with previous spectroscopic data from Simmerer et al. (2013) and Mucciarelli et al. (2015), and found that stars with variable behavior show larger spreads in metallicity, while the abundances of nonvariable stars are closer to the mean value of the cluster. As suggested by some authors, this result evidences that a larger iron spread is related to stellar variability. Recently, Cortés et al. (2023) performed a deep period analysis in 258 giant stars of NGC 3201, increasing the sample from Llancaqueo Albornoz et al. (2021).

In this work, we further expand the sample of stars provided by Llancaqueo Albornoz et al. (2021) and Cortés et al. (2023), presenting the analysis of 368 light curves—184 for V filter and 184 for I filter—of 184 stars from the globular cluster NGC 3201 within the magnitude range $V = 16–17$. Section 2 presents the information of the data utilized in this work. In Section 3 we explain the methodology and steps employed to search for variability in our sample. Section 4 shows our analysis of the stellar variability of the stars. Finally, in Section 5 we present our summary and conclusions obtained from this work.

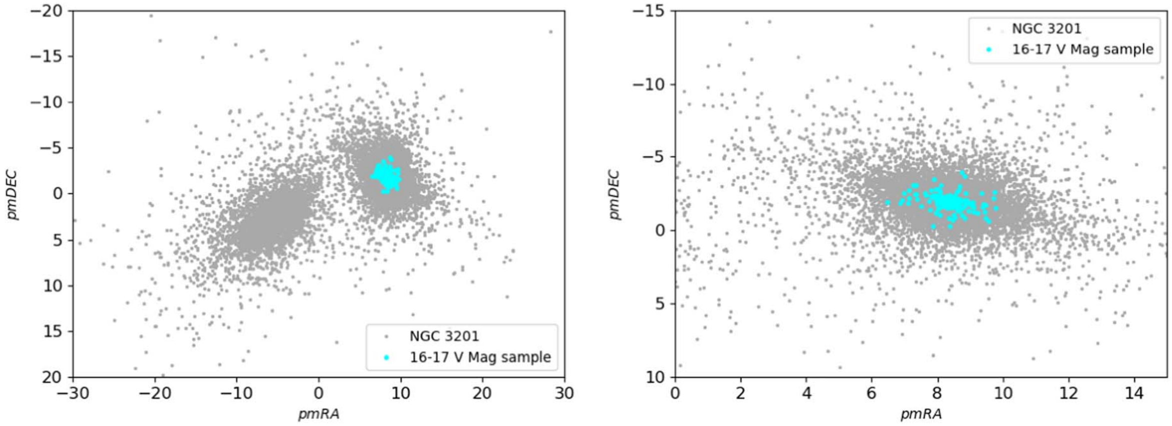

Figure 1. Proper motion on R.A. (pmR.A.) and decl. (pmdecl.) for NGC 3201 stars. The gray dots represent the Gaia data and the cyan dots are the stars of our sample which were matched with Gaia data. The right panel shows a closer look of the right group of stars in left panel.

2. Data

We worked with a sample of 368 light curves from globular cluster NGC 3201 stars. The data were originally published by Arellano Ferro et al. (2014) and provided by J.A. Ahumada, from the 2.15 m telescope at the Complejo Astronómico El Leoncito, San Juan, Argentina, on 2013 March 19–22. The detector used was a Roper Scientific back-illuminated CCD of 2048×2048 pixels, with a scale of $0\farcs15\ \mathrm{pix}^{-1}$ and a field of view of $5.1 \times 5.1\ \mathrm{arcmin}^2$ approximately. The data reduction and transformation to the *VI* standard system are presented by Arellano Ferro et al. (2014) in their Sections 2.2 and 2.3.

The sample analyzed consisted of Johnson–Kron–Cousins photometric systems *V* and *I*. The sample was selected through the color–magnitude diagram (CMD) with a magnitude between 16 and 17 in the *V* filter, with a total of 190 targets. 6 out of the 190 stars in this range have been analyzed by Arellano Ferro et al. (2014). We studied 184 stars that, according to their position in the CMD of this cluster, correspond to subgiant branch (SGB) and blue stragglers (BSS) stars.

The light curves contained 142 epochs in the *V* filter and 145 in the *I* filter, including the magnitude for each epoch, but three observations were affected by bad photometry in the *I* band. Therefore they were removed in each light curve as in Llancaqueo Albornoz et al. (2021). Moreover, seven stars had fewer epochs in the *I* filter, and 5 had fewer epochs in the *V* filter. It should be noted that each star in our sample has light curves in both filters, R.A. and decl., mean magnitudes in *V* and *I* filters, and $V - I$ color.

For further analysis, we needed to establish the membership of the cluster for these 184 stars. To do this, we obtained positions (R.A. and decl.) and proper motion (pmR.A. and pmdecl.) in the cluster FOV from the Gaia Mission Data Release 3 (Gaia Collaboration et al. 2016, 2023) public archive, and matched them with those corresponding to our photometric data using the Tool for OPerations on Catalogues And Tables (Taylor 2005). This match was made considering a maximum error of 2″, identifying 166 out of 184 targets which turned out to be all members (see Figure 1).

The light curve file data for each star analyzed is shown in Table 1, including standard magnitude, uncertainty, and internal errors for each filter.

Table 1
Sample Time Series for *V* and *I* Filters of Each Star

Star	Filter	HJD (day)	M_{std} (mag)	$\sigma_{M_{\mathrm{std}}}$ (mag)	σ_{int} (mag)
N° 1	*V*	2456371.52285	16.49470	0.0072	0.00389
N° 1	*V*	2456371.52598	16.53168	0.0075	0.00380
…	…	…	…	…	…
N° 1	*V*	2456372.54660	16.44897	0.0072	0.00317
N° 1	*V*	2456372.54918	16.44199	0.0071	0.00308
N° 1	*I*	2456371.51722	15.30581	0.0085	0.00502
N° 1	*I*	2456371.51971	15.27852	0.0089	0.00422
…	…	…	…	…	…
N° 2	*V*	2456371.52285	16.99843	0.0060	0.00568
N° 2	*V*	2456371.52598	16.99837	0.0059	0.00529
…	…	…	…	…	…
N° 2	*I*	2456371.51722	16.81257	0.0071	0.01803
N° 2	*I*	2456371.51971	16.78511	0.0070	0.01439
…	…	…	…	…	…
N° 20	*V*	2456371.52285	16.15610	0.0067	0.00280
N° 20	*V*	2456371.52598	16.15220	0.0067	0.00243
…	…	…	…	…	…
N° 20	*V*	2456373.51524	16.16589	0.0068	0.00293
N° 20	*V*	2456373.51708	16.16571	0.0067	0.00288
N° 20	*I*	2456371.51722	15.07340	0.0079	0.00401
N° 20	*I*	2456371.51971	15.06903	0.0079	0.00353
…	…	…	…	…	…

Note. This is a representative extract from the full table, which is available at the CDS.

3. Search for Variability

To determine which stars in our sample presented variability, we applied generalized Lomb–Scargle (GLS; Zechmeister & Kürster 2009) and phase dispersion minimization (PDM; Stellingwerf 1978) methods. These methods provide us periodograms to visualize periodic signals representing possible periods of our stars. To complement this analysis, we also applied a statistical test introduced by Llancaqueo Albornoz et al. (2021) and Cortés et al. (2023) as a significance test. In our looking for variability, we did not visualize nonperiodic variable stars.

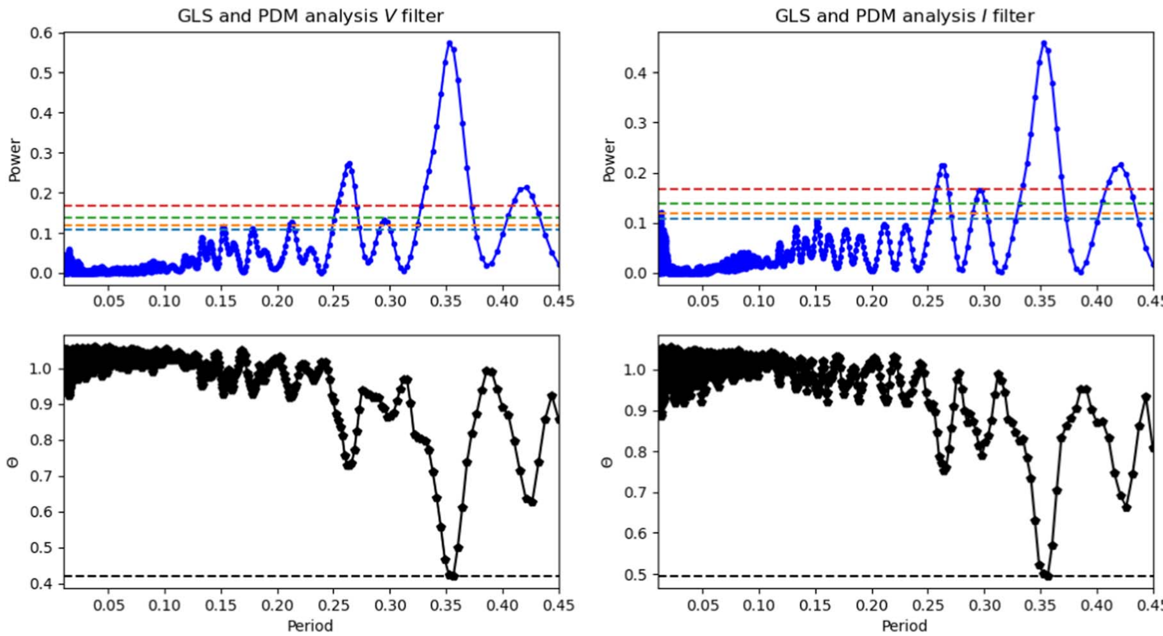

Figure 2. Periodograms for the star N° 4 after the significance test. The left panels show the *V* filter for the GLS, and the right panels show the *I* filter. For the GLS periodograms (upper panels), the colored dashed lines represent different FAP levels (10% in blue, 5% in orange, 1% in green, and 0.1% in red). The bottom panels show the PDM periodograms, in which the black dashed line represents the lower value of Θ. According to the criteria described above, we choose a period of 0.352158 days for this variable star.

3.1. Periodogram Analysis

Our search for variability was performed through the GLS[5] and PDM[6] periodograms using the *PyAstronomy*[7] (PyA) package collection (Czesla et al. 2019) in *Python*.

GLS represents the periodic signal, which indicates our period candidates as local maxima in the plot. To compare every maximum and determine which are the reliable ones, the method defines confidence levels to ensure our signal is not accidental or noise, called false alarm probability (FAP). The maxima have to be higher than a 0.1% level, indicating that there is a 0.1% of probability this height was reached by error. Unlike GLS, PDM aims to minimize the variance of the data, which is represented by a parameter Θ. With this method, the periodic signal would be represented by local minima. Hence, the lower the curve, the higher the confidence in the period.

We used both methods because GLS is optimized to identify a periodic signal in a sinusoidal shape in the light curves and PDM is useful for nonsinusoidal variations of data sets with few irregularly spaced observations, as is the case with the data used in this research.

Therefore, our script applies GLS and PDM methods, generating outputs for both periodograms in both bands (see Figure 2). In addition, it gives us information on the higher-amplitude period in days, its amplitude, the errors of these measurements, and the root mean square (RMS) of the data. We also used the PDM task from IRAF. This task uses the light-curve data as input and outputs a periodogram, independent of our script, helping us to compare the periodograms obtained through our script and IRAF. In order to determine the best period, we analyzed all the possible periods shown in the periodogram, recording in the article the period with a significant peak.

Finally, to determine which period was correct, we applied the following criteria:

1. The period in both periodograms and in both filters must be similar.
2. The highest peak indicated as the candidate period in the GLS periodogram for both bands must be above 0.1% FAP level.
3. The amplitude with the error of the candidate period has to be higher than the RMS of the data.
4. The candidate periods obtained with PDM and GLS must be similar in both filters.

From this analysis, we selected 20 out of the 184 stars as variable candidates.

3.2. Significance Test

In this section, we applied the significance test employed by Llancaqueo Albornoz et al. (2021) and Cortés et al. (2023) to classify the 20 candidate variable stars as variable, possible, dubious, or nonvariable.

We define a significance parameter S as:

$$S = \frac{\sigma_{\rm var} - \sigma_{\rm non-var}}{\sqrt{{\rm err}^2_{\sigma_{\rm var}} + {\rm err}^2_{\sigma_{\rm non-var}}}}. \quad (1)$$

We calculated $\sigma_{\rm var}$, $\sigma_{\rm non-var}$ and their error through the following steps:

(1) We calculated ΔM, which is the difference between the magnitude on each epoch and the mean magnitude for each one of the 184 stars;
(2) We obtained the variance for each filter and for each one of the 184 stars $\sigma_M = \sqrt{\frac{\sum \Delta M^2}{N-1}}$ and its error $err_\sigma = \frac{\sigma_M}{\sqrt{2N}}$;

[5] https://pyastronomy.readthedocs.io/en/latest/pyTimingDoc/pyPeriodDoc/gls.html
[6] https://pyastronomy.readthedocs.io/en/latest/pyTimingDoc/pyPDMDoc/classes.html
[7] https://pyastronomy.readthedocs.io/en/latest/

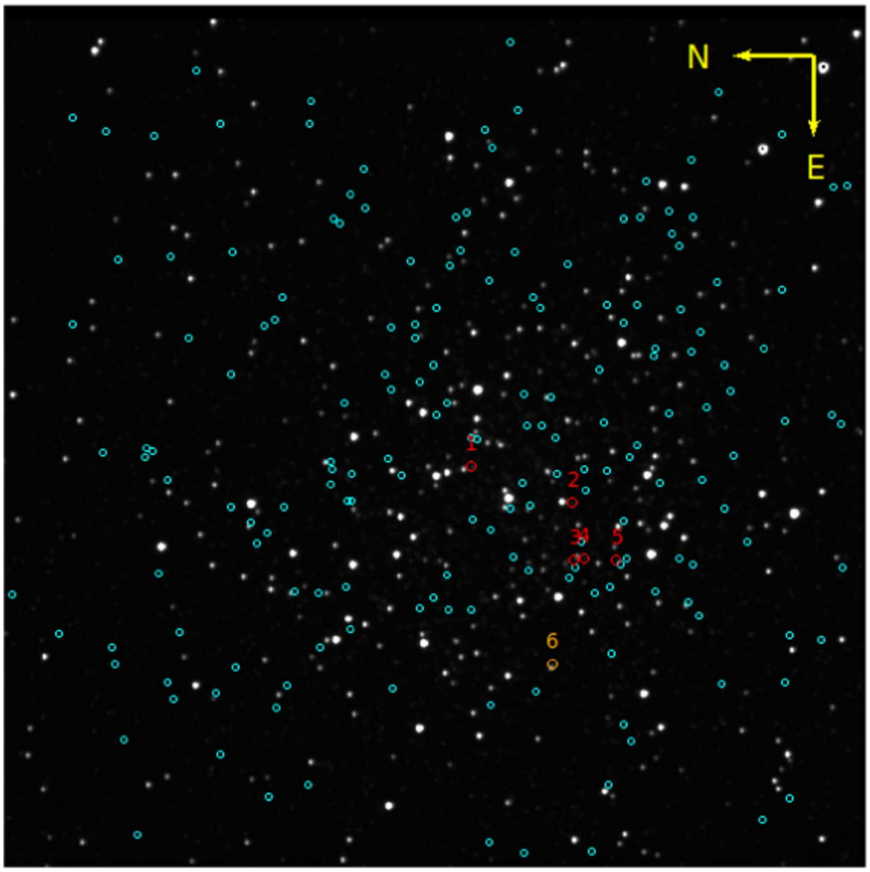

Figure 3. Finding chart of the area of NGC 3201 of the 184 stars studied. Red and orange circles mark the stars considered as variables and possible variable, respectively, with the ID shown in Table 2. The complete sample of stars analyzed is represented with cyan circles. The area shown is 5$''$.4 × 5$''$.4 and is centered in $\alpha = 10^h17^m34^s.87$, $\delta = -46°24'17''9$ (J2000)

Table 2
Classification and the Significance Values For Six Stars

ID (CMD)	ID (Gaia DR3)	R.A. (J2000)	Decl. (J2000)	$\langle V \rangle$ (mag)	$\langle I \rangle$ (mag)	$V - I$	S_V	S_I	Classification
1	5413575619690180352	10:17:36.028	−46:24:30.48	16.46498	15.29121	1.17377	13.775	11.068	Variable
2	5413575623988741248	10:17:37.488	−46:25:05.95	16.96860	16.78130	0.18730	3.291	11.065	Variable
3	5413575555269309696	10:17:39.445	−46:25:05.22	16.74507	15.80698	0.93809	16.093	15.582	Variable
4	5413575555269308544	10:17:39.420	−46:25:08.81	16.88844	15.83483	1.05360	14.408	10.900	Variable
5	5413575555275128960	10:17:39.571	−46:25:20.14	16.76369	16.09046	0.67323	3.587	6.153	Variable
6	5413575658348783232	10:17:43.006	−46:24:55.16	16.73648	15.62412	1.11236	6.718	−4.337	Possible variable

(3) We separated σ_M and err_σ for variable ($\sigma_{\rm var}$ and $err_{\sigma_{\rm var}}$) and nonvariable stars ($\sigma_{\rm non-var}$ and $err_{\sigma_{\rm non-var}}$);
(4) Finally, we replaced the values obtained in point (3) in the equation of significance S, defined above.

This test allowed us to know if the star could be considered a variable, nonvariable, possible, or dubious variable star. To carry out the classification, we follow the following criteria:

1. If $S_V > 3$ and $S_I > 3$, the star is considered as variable.
2. If $S > 3$ in only one filter, the star is considered as possible variable.
3. If $S_V < 2$ and $S_I < 2$, the star is considered as nonvariable.
4. If $2 < S < 3$ in one or both filters, the star is considered as dubious variable, and a further analysis have to be done to the confirmation.

From this new analysis, 14 stars were considered as nonvariables, five as variables, and one as a possible variable (Figure 3). Table 2 shows the significance values for the variable and possible variable stars, with their coordinates (R. A. and decl.), ID from GAIA DR3, the mean magnitudes in V and I bands, and the classification according to the previously present criteria.

4. Analysis For Stellar Variability

Once the significance test had been done, we analyzed if our stars could resemble some cataloged variable star. For this, we compared the period, amplitude, position in the CMD (Figure 4) and the shape of the phased light curve (Figure 5) of our stars (Table 3) with known variables, using the General Catalogue of

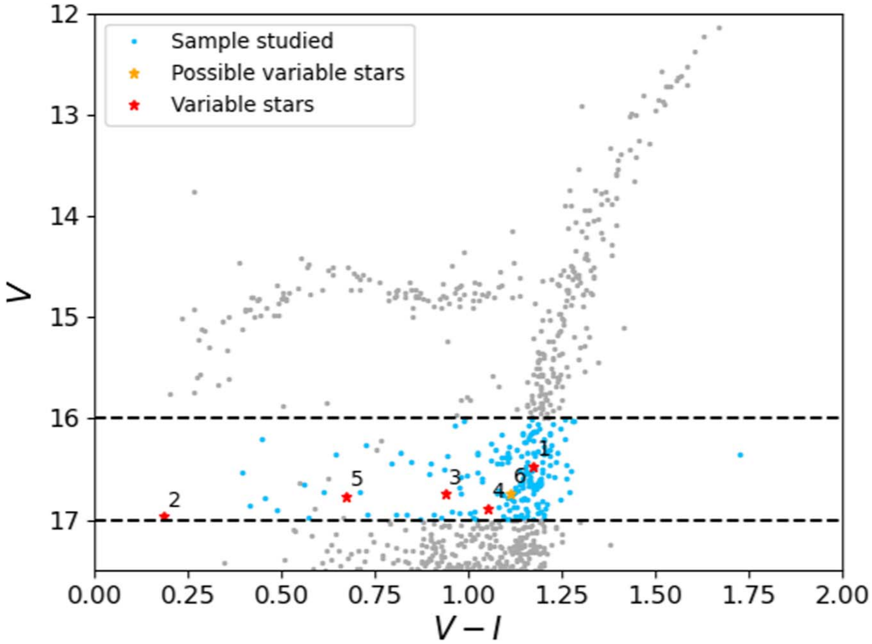

Figure 4. NGC 3201 color–magnitude diagram. The complete sample of stars analyzed is shown as cyan dots. Red and orange stars represent those stars considered as variables and possible variables, respectively.

Table 3
Final Parameters for Stars Classified as Variable and Possible Variable from the Significance Test

ID	Variability	P_V (days)	$P_{V\mathrm{err}}$ (days)	A_V (mag)	$A_{V\mathrm{err}}$ (mag)	PI (days)	$PI\mathrm{err}$ (days)	A_I (mag)	$A_{I\mathrm{err}}$ (mag)	CMD Position
1	Variable	0.530	0.003	0.203	0.006	0.530	0.003	0.122	0.003	SGB
2	Variable	0.544	0.005	0.042	0.001	0.535	0.006	0.100	0.004	BSS
3	Variable	0.538	0.002	0.874	0.017	0.538	0.003	0.590	0.012	SGB/YSS
4	Variable	0.352	0.002	0.224	0.008	0.352	0.002	0.095	0.004	SGB
5	Variable	0.332	0.003	0.033	0.001	0.332	0.005	0.037	0.002	BSS/YSS
6	Possible variable	0.336	0.002	0.048	0.002	0.332	0.004	0.020	0.001	SGB

Variable Stars (Samus'et al. 2017) as a reference. According to their position, our variable stars belong to the SGB and BSS regions and in between (yellow stragglers; YSS).

1. *Star N° 1*: the star was found to have a period of 0.53 days and an amplitude of 0.20 magnitudes in *V* filter. The phased light curve presents a rapid increase followed by a very slight decrease, almost flat, and a faster drop in brightness. This variable star is located in the SGB as shown in the CMD (Figure 4). No cataloged variable stars were found with these characteristics.
2. *Star N° 2*: the star presented a variation in its magnitude in *V* filter of 0.04 magnitudes in 0.54 days. As *Star N° 1*, it presents a rise in its brightness, maintaining its maxima and decreasing again. In the *I* band, the increase and decrease are faster than in *V* filter. Its phased light curve could resemble *Star N° 4* presented in Llancaqueo Albornoz et al. (2021), but the period, amplitude, and evolutionary state are different. According to the CMD (Figure 4), our star is positioned in the blue stragglers region, while *Star N° 4* from Llancaqueo Albornoz et al. (2021) is in the lower part of the giant branch. No cataloged variable stars were found with these characteristics.
3. *Star N° 3*: the star presents an amplitude in *V* band of 0.87 magnitudes with a period of 0.54 days and appears slightly away from the SGB of the cluster, as shown in Figure 4. Unlike *Star N° 1* and *Star N° 2*, the phased light curve presents a very slow decrease in magnitude at the bottom of the curve, followed by a rapid increase and a slighter second decrease. Type-ab RR Lyrae present this behavior, and could also have similar periods and amplitudes; but those stars belong to the HB and ours to SGB. We did not find any cataloged variable star with these characteristics.
4. *Star N° 4*: This variable star is located in the subgiant branch region (Figure 4). The phased light curve is similar to *Star N° 3* but has no gaps and less abrupt changes. It has a period of 0.35 days and an amplitude of 0.22 magnitudes in *V* filter. No cataloged variable stars were found with these characteristics.
5. *Star N° 5*: this star presented a period of 0.33 days and an amplitude of 0.03 magnitudes in the *V* band. The phased light curve in the *V* filter shows a continuous decrease in magnitude followed by a rapid increase. In the *I* filter, the magnitude decreases very slowly, but some points are lower than most of them, possibly due to dispersion. Based on these parameters and according to the position

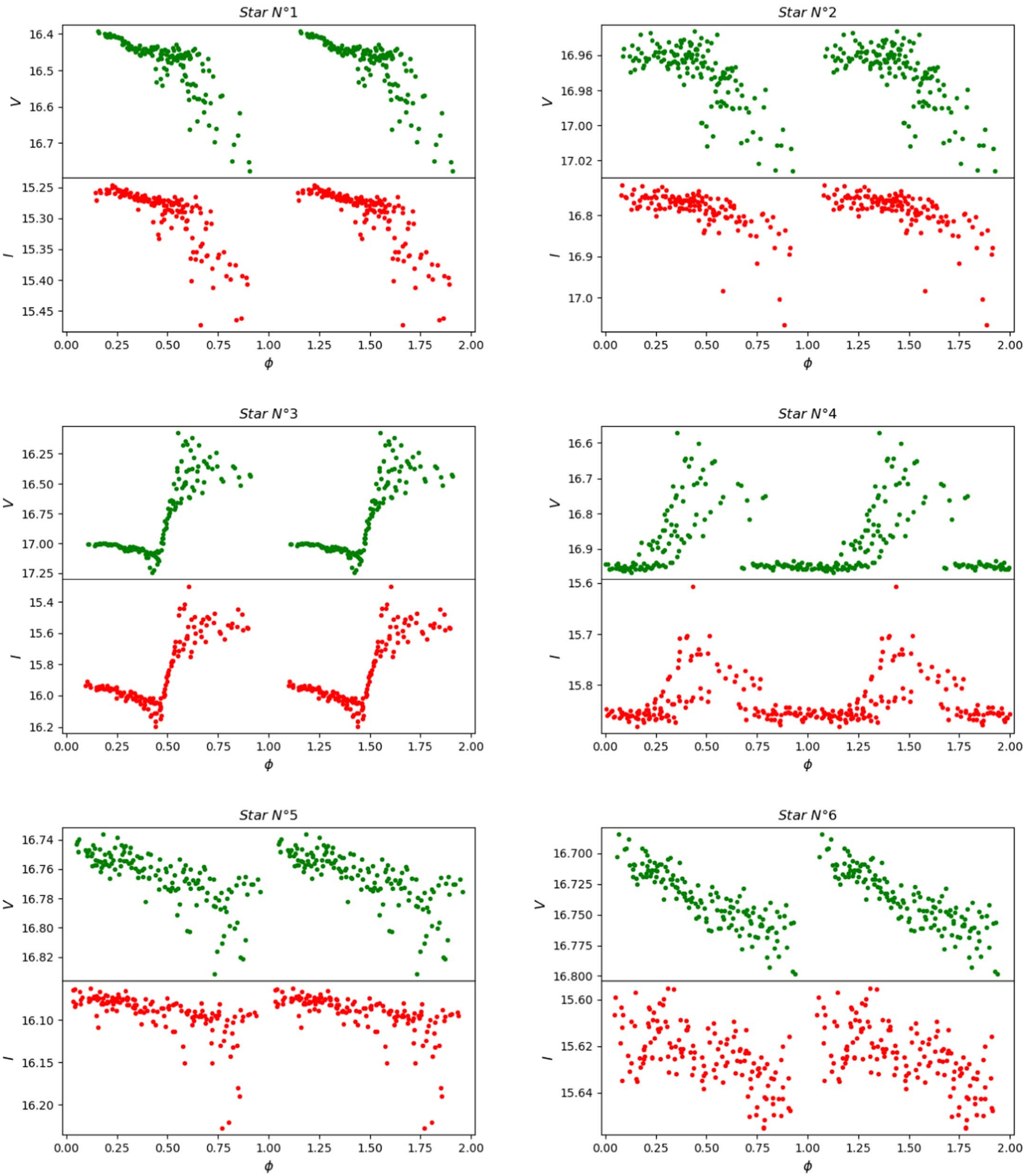

Figure 5. Phased light curves for stars considered as variable and possible variable stars (Table 2) according to the significance test. For each star, the top panel corresponds to the phased light curve in V band and the bottom panel to the I band.

in the CMD (Figure 4) this star is located in yellow/blue stragglers. No cataloged variable stars were found with these characteristics.

6. *Star N° 6*: such as *Star N° 5* but more evident, the phased light curve presents a slow decrease and a fast increase in magnitude. It has a period of 0.34 days and a variation in V magnitude of 0.05 magnitudes. This possible variable star is positioned in the Subgiant Branch (Figure 4). As *Star N° 5*, no cataloged variable stars were found with these characteristics.

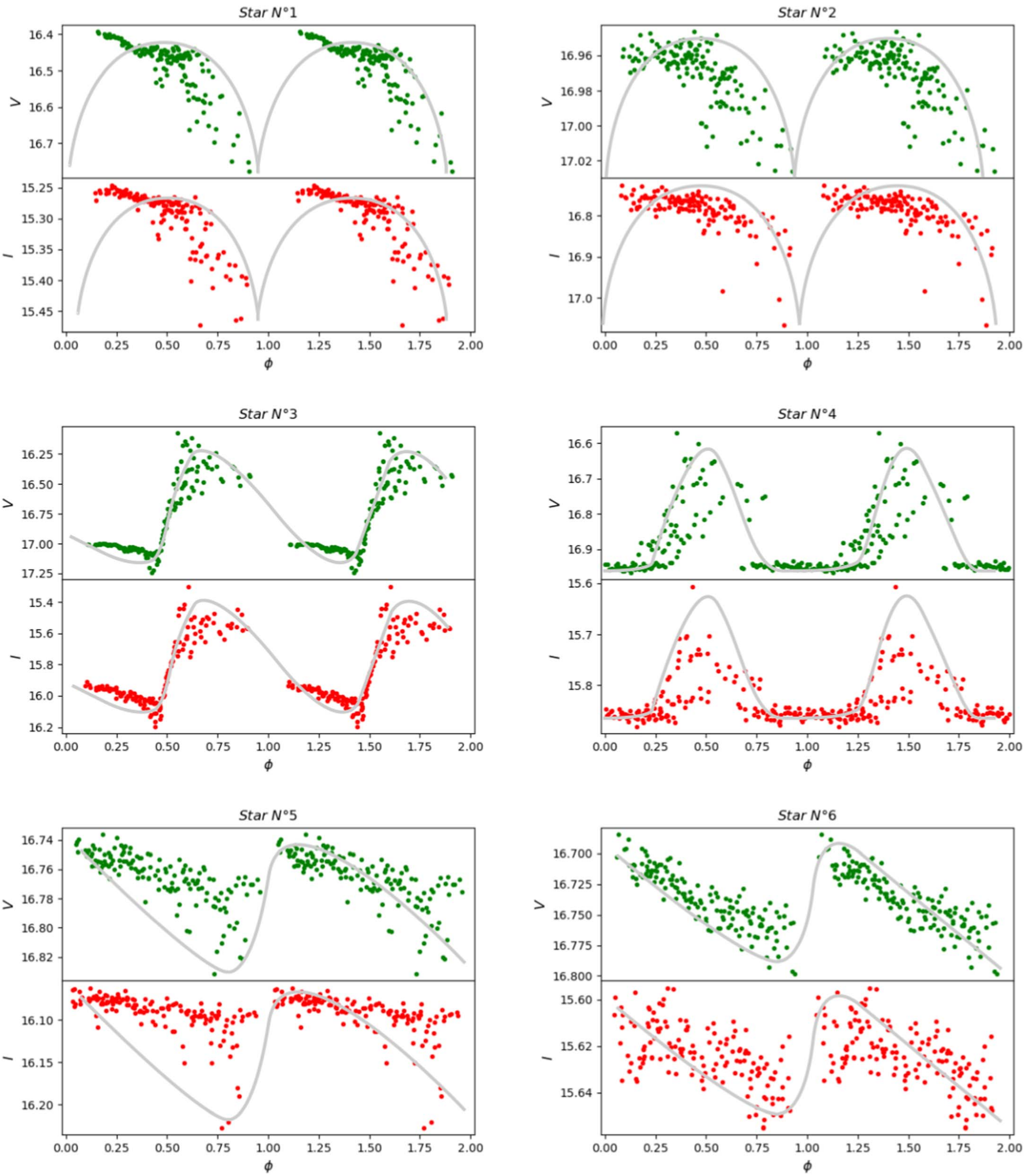

Figure 6. Tendencies followed by the phased light curves for the variables and the possible variable stars according to the classification made by Cortés et al. (2023).

We also compared our phased light curves with those studied by Cortés et al. (2023). They classified their variable and possible variable stars according to the shape of their phased light curves, resulting in four different groups. This comparison was made to better understand the shape of the phased light curves in our sample, but the range of magnitudes and the evolutionary stage for the stars they studied are different than ours. The shapes of our phased light curves according to the classification made by Cortés et al. (2023) are shown in Figure 6.

1. *Star N° 1* and *Star N° 2* flattens in the upper part of the phased light curve, after a rapid increase and is followed by a similar decrease in their magnitudes. They resemble the shape of the light curves from Group 4 by Cortés et al. (2023), especially *Star N° 88* and *Star N° 27*, respectively, from their sample. *Star N° 27* also have similar period to *Star N° 2* from our sample.
2. *Star N° 4* phased light curve resembles Group 1 stars, which phased light curves are sharp at the upper part of it, unlike those from Group 4, and are very symmetrical. It could resemble *Star N° 42* observed by Cortés et al. (2023), but flatter at the lower part of the curve. Its period is similar, but its amplitude and position in the CMD are not.
3. Phased light curves for *Star N° 3*, *Star N° 5*, and *Star N° 6* present a rapid increase and a slower decrease in their magnitude, just as Group 2 stars. *Star N° 3* looks like *Star N° 13* from Cortés et al. (2023), which is also similar to *Star N° 1* from Llancaqueo Albornoz et al. (2021), but its period and position in the CMD does not match. *Star N ° 5* and *Star N° 6* resembles *Star N° 7* and *Star N° 20*, respectively, from Cortés et al. (2023) specially in the shape of their light curves. The periods and amplitudes are also similar, but they belong to other regions in the CMD.

Stars of our sample are unlike those of any known variability types. It is imperative that we supplement our research with spectroscopic analysis to obtain conclusive results.

5. Conclusion

We analyzed the light curves in *V* and *I* filters for 184 stars in the globular cluster NGC 3201 with magnitudes between 16 and 17 in the *V* band, in order to search for variability and expand the sample of a new type of variable stars in this cluster, complementing the work made by Llancaqueo Albornoz et al. (2021) and Cortés et al. (2023). For this, we used generalized Lomb–Scargle and phase dispersion minimization methods to inspect the variability of our sample by their periodograms and applied a statistical test introduced by Llancaqueo Albornoz et al. (2021) that quantifies the magnitude changes over time for each star. After this, five stars were considered as variables and one was considered as a possible variable.

Once the variables and possible variable stars were found, we compared them with known variable stars. These six stars, located in between the subgiant branch and blue stragglers regions, appeared to have periods between 0.33 and 0.54 days and amplitudes between 0.03 and 0.87 mag in the *V* filter. Based on their periods, amplitudes, position in the color–magnitude diagram, and shape of their phased light curves, none of the stars in our sample resembles cataloged variable stars. We compared our sample with pulsating, rotating, and close binary variable stars, because eruptive and cataclysmic variables have nonperiodical variations, and eclipsing binaries have very recognizable phased light curves.

Because variability could be complex and stars may present more than one cause of variation, we propose to complement this work with spectroscopic analysis. This would provide us a better characterization of our stars.

Furthermore, the similarity in some periods, amplitudes, and shapes of phased light curves between the giant stars studied by Llancaqueo Albornoz et al. (2021) and Cortés et al. (2023), and the early evolved stars studied in this paper could suggest that the giant variable stars they found are evolved SBG, YSS, and BSS variable stars. We should extend this study to stars that have recently left the main sequence of the cluster, i.e., stars from the turnoff point, looking for similar characteristics.

Acknowledgments

C.C.C. gratefully acknowledges the support provided by MINEDUC ADAIN project TAL2293. S.V. gratefully acknowledges the support provided by Fondecyt reg. n. 1220264. S.V. gratefully acknowledges also the support provided by the ANID BASAL projects ACE210002 and FB210003. This work is based on data acquired at Complejo Astronómico El Leoncito, operated under agreement between the Consejo Nacional de Investigaciones Científicas y Técnicas de la República Argentina and the National Universities of La Plata, Córdoba and San Juan. Furthermore, this work made use of the PyAstronomy package collection and we are thankful at the PyA group for answering our doubts regarding their packages.

This work has made use of data from the European Space Agency (ESA) mission Gaia (https://www.cosmos.esa.int/gaia), processed by the Gaia Data Processing and Analysis Consortium (DPAC; https://www.cosmos.esa.int/web/gaia/dpac/consortium). Funding for the DPAC has been provided by national institutions, in particular the institutions participating in the Gaia Multilateral Agreement.

ORCID iDs

D. Ulloa-Solís https://orcid.org/0009-0009-3715-1578
C. C. Cortés https://orcid.org/0000-0002-5003-3762
S. Villanova https://orcid.org/0000-0001-6205-1493
Á. Llancaqueo Albornoz https://orcid.org/0000-0003-3131-2464
J. A. Ahumada https://orcid.org/0000-0002-7091-5025
C. Parisi https://orcid.org/0000-0001-9382-3986

References

Arellano Ferro, A., Ahumada, J. A., Calderón, J. H., & Kains, N. 2014, RMxAA, 50, 307
Carretta, E., Bragaglia, A., Gratton, R., & Lucatello, S. 2009a, A&A, 505, 139
Carretta, E., Bragaglia, A., Gratton, R. G., et al. 2009b, A&A, 505, 117
Clement, C. M., Muzzin, A., Dufton, Q., et al. 2001, AJ, 122, 2587
Cortés, C. C., Llancaqueo Albornoz, Á., Villanova, S., Ahumada, J. A., & Parisi, C. 2023, AJ, 166, 95
Czesla, S., Schröter, S., Schneider, C. P., et al., 2019 PyA: Python astronomy-related packages, Astrophysics Source Code Library, ascl:1906.010
Eggen, O. J. 1973, ApJ, 184, 793
Eggen, O. J. 1977, ApJ, 213, 767
Gaia Collaboration, Prusti, T., de Bruijne, J. H. J., et al. 2016, A&A, 595, A1
Gaia Collaboration, Vallenari, A., Brown, A. G. A., et al. 2023, A&A, 674, A1
Gonzalez, G., & Wallerstein, G. 1998, AJ, 116, 765
Gratton, R., Sneden, C., & Carretta, E. 2004, ARA&A, 42, 385
Harris, W. E. 1996, AJ, 112, 1487
Kaluzny, J., Rozyczka, M., Thompson, I. B., et al. 2016, AcA, 66, 31
Layden, A. C., & Sarajedini, A. 2003, AJ, 125, 208
Llancaqueo Albornoz, Á., Villanova, S., Cortés, C. C., Ahumada, J. A., & Parisi, C. 2021, AJ, 161, 76
Minniti, D., Lucas, P. W., Emerson, J. P., et al. 2010, NewA, 15, 433
Mucciarelli, A., Lapenna, E., Massari, D., Ferraro, F. R., & Lanzoni, B. 2015, ApJ, 801, 69
Muñoz, C., Geisler, D., & Villanova, S. 2013, MNRAS, 433, 2006

Muñoz, C., Geisler, D., Villanova, S., et al. 2018, A&A, 620, A96
Saito, R. K., Hempel, M., Minniti, D., et al. 2012, A&A, 537, A107
Samus', N. N., Kazarovets, E. V., Durlevich, O. V., Kireeva, N. N., & Pastukhova, E. N. 2017, ARep, 61, 80
Simmerer, J., Ivans, I. I., Filler, D., et al. 2013, ApJL, 764, L7
Stellingwerf, R. F. 1978, ApJ, 224, 953
Taylor, M. B. 2005, in ASP Conf. Ser. 347, Astronomical Data Analysis Software and Systems XIV, ed. P. Shopbell, M. Britton, & R. Ebert (San Francisco, CA: ASP), 29
Zechmeister, M., & Kürster, M. 2009, A&A, 496, 577